Developmental Biology 341 (2010) 488–498

Contents lists available at ScienceDirect

Developmental Biology

journal homepage: www.elsevier.com/developmentalbiology

Genomes & Developmental Control

Additive and global functions of *HoxA* cluster genes in mesoderm derivatives

Nicolas Di-Poï [a], Ute Koch [b], Freddy Radtke [b], Denis Duboule [a,b,*]

[a] National Research Center "Frontiers in Genetics", Department of Zoology and Animal Biology, University of Geneva, Sciences III, 1211 Geneva 4, Switzerland
[b] ISREC, School of Life Sciences, Federal Institute of Technology (EPFL), 1015 Lausanne, Switzerland

ARTICLE INFO

Article history:
Received for publication 29 December 2009
Revised 9 March 2010
Accepted 9 March 2010
Available online 18 March 2010

Keywords:
HoxA
HoxD
Mesoderm
Hematopoiesis
Skeleton
Organs
Skin

ABSTRACT

Hox genes encode transcription factors that play a central role in the specification of regional identities along the anterior to posterior body axis. In the developing mouse embryo, *Hox* genes from all four genomic clusters are involved in range of developmental processes, including the patterning of skeletal structures and the formation of several organs. However, the functional redundancy observed either between paralogous genes, or among neighboring genes from the same cluster, has hampered functional analyses, in particular when synergistic, cluster-specific functions are considered. Here, we report that mutant mice lacking the entire *HoxA* cluster in mesodermal lineages display the expected spectrum of postnatal respiratory, cardiac and urogenital defects, previously reported for single gene mutations. Likewise, mild phenotypes are observed in both appendicular and axial skeleton. However, a striking effect was uncovered in the hematopoietic system, much stronger than that seen for *Hoxa9* inactivation alone, which involves stem cells (HSCs) as well as the erythroid lineage, indicating that several *Hoxa* genes are necessary for normal hematopoiesis to occur. Finally, the combined deletions of *Hoxa* and *Hoxd* genes reveal abnormalities in axial elongation as well as skin morphogenesis that are likely the results of defects in epithelial–mesenchymal interactions.

Introduction

In most vertebrates, mammalian *Hox* genes are organized into four separate chromosomal clusters (*HoxA*, *HoxB*, *HoxC* and *HoxD*), which are further divided into 13 groups of paralogy, based on both sequence similarity and respective position along the gene clusters. These genes are expressed in a spatio-temporal manner which reflects their physical positions along the clusters (Gaunt et al., 1988; Duboule and Dolle, 1989; Graham et al., 1989) and play a central role in the specification of regional identities along the anterior to posterior body axis (McGinnis and Krumlauf, 1992). In the developing mouse embryo, *Hox* genes are involved in a number of other developmental processes, including patterning of skeletal structures as well as formation of several organ systems. In particular, phenotypes of single and compound mouse mutants for *Hoxa* and *Hoxd* genes have revealed a crucial role for these genes in the development of mesoderm-derived tissues including limbs, the axial skeleton and kidneys (Di-Poi et al., 2007; Kmita et al., 2005; McIntyre et al., 2007).

These studies also revealed that *Hox* genes have retained partially overlapping expression patterns, accompanying a considerable functional redundancy either between paralogous genes, adjacent genes or even non-paralogous genes in separate clusters. This suggests that these genes likely function as members of large genetic networks, with complex dose-dependent contributions (Davis and Capecchi, 1996; de la Cruz et al., 1999; Magnusson et al., 2007a). For example, hematopoietic cells from both mouse and human bone marrow (BM) express the majority of *Hox* genes located on the *HoxA*, *HoxB* and *HoxC* clusters, yet loss-of-function mutations resulted in very mild hematopoietic phenotypes, except for the case of *Hoxa9* (Lawrence et al., 1996; McGonigle et al., 2008).

In such a buffered genetic system, multiple and combined loss of functions are often necessary to elicit significant functional disorders. Such combined inactivations can be vertical, i.e. they can involve paralogous genes from different, possibly all gene clusters, in which case they can reveal the function of a particular paralogy group during development. Redundancy between such paralogous genes indicates a conservation of both the gene function and the expression specificity (e.g. *Hox10* genes in the axial skeleton; Wellik and Capecchi, 2003). Conversely, a horizontal approach, the deletion of an entire gene cluster, will reveal whether neighboring genes share particular functions, i.e. whether they are coordinately regulated into the same tissues at the same time. This may indicate the presence of a 'cluster-specificity', resulting from the existence of a global regulation, which may or may not be shared between gene clusters (Duboule, 2007). The deletion of *HoxA* cluster genes in developing neural crest cells illustrates the presence of such a global regulation, absent from the *HoxD* cluster (Minoux et al., 2009), much in the same way the deletion of *Hoxd* genes revealed a global limb-specific regulation

* Corresponding author. National Research Center "Frontiers in Genetics", Department of Zoology and Animal Biology, University of Geneva, Sciences III, 1211 Geneva 4, Switzerland. Fax: +41 22 379 6795.
E-mail addresses: denis.duboule@unige.ch, denis.duboule@epfl.ch (D. Duboule).

0012-1606/$ – see front matter © 2010 Elsevier Inc. All rights reserved.
doi:10.1016/j.ydbio.2010.03.006

(Spitz et al., 2001). In other cases, horizontal deletions of multiple genes resulted mostly in additive phenotypes (Suemori and Noguchi, 2000; Medina-Martinez et al., 2000).

Genes belonging to the *HoxA* cluster are broadly expressed within the hindbrain, neural tube and mesodermal layers. Functional analyses demonstrated their separate implications into hematopoiesis, as well as during the patterning of several tissues such as the limbs, the lungs, the kidneys, the heart and the genital system (Aubin et al., 1997; Chisaka and Capecchi, 1991; Fromental-Ramain et al., 1996b; Lawrence et al., 2005; Zhao and Potter, 2002). In order to assess the combined functional contributions of all 11 mouse *Hoxa* genes to the development of mesodermal tissues, we used a conditional *HoxA* cluster allele in conjunction with a *T/brachyury* promoter (*T-Cre*) driving *Cre* recombinase deleter strain. This promoter is active early on in the primitive streak and migrating mesoderm cells and thus induces the deletion of *Hoxa* genes in the different mesodermal lineages including the paraxial, intermediate and lateral plate mesoderm, starting from early developmental stages (Clements et al., 1996; Perantoni et al., 2005).

We report that mutant mice lacking mesodermal expression of all *Hoxa* genes survive until birth and succumb from a spectrum of defects, including growth retardation and respiratory, cardiac and hematopoietic abnormalities. While the conditional deletion of the whole *HoxA* cluster reproduces most of the phenotypes already reported for single *Hoxa* gene mutations, our approach revealed severe hematopoietic defects in spleen, bone marrow and thymus, indicating overlapping functions of multiple *Hoxa* genes in these tissues. Finally, the conditional deletion of the *HoxA* cluster, combined with deletions within the *HoxD* cluster, revealed a strong phenotype in early embryonic skin development, not reported so far for a *Hox* mutation, whereas a comparatively weak phenotype was observed in the axial skeleton, reminiscent from the effects induced by single *HoxA* or *HoxD* cluster deletions.

Materials and methods

Mouse strains

The generation of floxed (A^{flox}) and deleted (A^{-}) *HoxA* cluster alleles was described previously (Kmita et al., 2005). Mice mutant for the *HoxD* cluster were produced by targeted meiotic recombination (Del(1–13), Zakany et al. 2001) or *loxP/Cre* mediated site-specific recombination in ES cells (Del(4–13), Zakany and Duboule, 1999; Del (4–11), Zacchetti et al., 2007). Transgenic lines expressing *Cre* recombinase under the control of the primitive streak regulatory elements of the *T* promoter (Clements et al., 1996), or mesodermal (msd) regulatory elements of *Delta1* promoter (Beckers et al., 2000) were provided by A. Gossler. The *Rosa26R Cre* reporter (*R26R*) strain was described previously (Soriano, 1999). All animals and embryos were genotyped by classical or quantitative real-time PCR (using SYBR green) on tail genomic DNA. The efficiency of *T-Cre* mediated recombination on genomic DNA was assessed through the disappearance of *Hoxa11*. B6.SJL-*Ptprc*^{a} mice (CD45.1^{+}) were purchased from the Jackson Laboratory, Bar Harbor, ME.

Histology, LacZ staining and skeletal preparation

For histological analyses, newborn mice were sacrificed and fixed for 5–7 days in Bouin's solution before alcohol dehydration and paraffin embedding. Whole mice were sectioned at 5 µm and stained with hematoxylin and eosin according to standard protocols. Whole mount histochemical detection of beta-galactosidase reporter activity in embryos or isolated organs was carried out by *LacZ* staining as described (Di-Poi et al., 2007). Skeletal stainings of embryos or newborn mice with Alizarin red and Alcian blue were carried out using standard procedures.

Generation of fetal liver chimeras

Fetal livers (FLs) from E12.5 or E13.5 embryos were individually isolated, and the genotype of single embryos was determined by PCR. Single-cell suspensions were prepared from FLs with the desired genotypes. A total of $2–3\times10^{6}$ FL cells were injected intravenously together with T cell depleted 5×10^{5} bone marrow cells from congenic CD45.1^{+} mice in a volume of 200 µl phosphate-buffered saline (PBS) into lethally irradiated congenic CD45.1^{+} recipients.

Antibodies and flow cytometry

Single-cell suspensions from bone marrow, thymus and spleen were prepared and stained for FACS analysis using standard protocols as previously described (Wilson et al., 2001). The antibodies used to analyze the hematopoietic and lymphoid lineages are listed below. The following monoclonal antibody conjugates were purchased from eBioscience (San Diego, CA): CD117 (c-kit, 2B8)–APC; Sca-1 (Ly6A/E, D7)–PECy5; B220 (RA3-6B2)–PECy5, –PECy7; TCRβ (H57-597)–FITC, –PECy7; CD135 (Flt3, A2F10)–PE; CD71 (Transferrin receptor, R17217)–PE; CD25 (IL-2R, PC61.5)–APC-Alexa750; CD34 (RAM34)–FITC; CD11b (Mac-1, M1/70)–PECy5, –PECy7; Ter119 (Ly76)–PECy7; CD19 (1D3)–PECy7; CD43 (Ly-48, S7)–Biotin; IgM (eB121-15F9)–APC; CD4 (L3T4, GK1.5)–PECy7; CD8α (53.6.7)–PECy7; Gr-1 (Ly-6G)–PECy7; TCRγδ (GL3)–PE and CD44 (PgP-1, IM7)–PE. Gr-1 (Ly-6G)–Alexa647 and CD8α (53.6.7)–Alexa647 were purified from hybridoma supernatants and conjugated following standard protocols. Alexa647 conjugates were prepared using the appropriate Alexa protein labelling kits (Invitrogen, Molecular Probes, Basel, Switzerland). Streptavidin-APC-Alexa750 (eBioscience) was used to reveal biotin conjugates. Fluorescence-activated cell sorter (FACS) analyses (7-color) were performed using CyAn™ADP analyzer (Beckman Coulter, Nyon, Switzerland). Data were analyzed using FlowJo software (Tree Start, Ashland, OR). The independent Student's *t*-test was used for all statistical analyses.

Results

Conditional deletion of the HoxA cluster in mesodermal lineages

As several *Hoxa* genes are expressed in overlapping regions of mesodermal origins during mouse development (see e.g. Kmita et al., 2005; Wellik and Capecchi, 2003), and also to overcome the early embryonic lethality caused by the functional ablation of *Hoxa13* (Fromental-Ramain et al., 1996b), we used a conditional *HoxA* cluster allele, flanked by *loxP* sites (*HoxA*^{flox} or A^{flox}; Fig. 1A and Kmita et al., 2005), in conjunction with deleter mice expressing the *Cre* recombinase under the control of *T/brachyury* promoter (*T-Cre*). This promoter is functional early on in mesodermal cells of the primitive streak, slightly before the onset of anterior *Hox* gene expression (Deschamps et al., 1999) and is thus active in virtually all mesodermal lineages including paraxial, intermediate and lateral plate mesoderm (Clements et al., 1996; Perantoni et al., 2005).

We first determined the efficiency of *T-Cre* mediated deletion of the 110 kb large *HoxA* cluster by quantitative PCR on genomic DNA. We compared mutants homozygous for a conditional *HoxA* deletion ($A^{c/c}$) with mice *trans*-heterozygous for both a full *HoxA* deletion (*HoxA*$^{-}$ or A^{-}) and the conditional allele (*HoxA*$^{c/-}$ or $A^{c/-}$). This latter combination exhibited a significantly higher and less variable efficiency of deletion (Fig. 1B) and was thus subsequently used for all phenotypic analyses (see below). Mutant mice lacking mesodermal expression of the *HoxA* cluster ($A^{c/c}$ and $A^{c/-}$) survived throughout embryonic development and were born following a Mendelian ratio (data not shown). However, most of the $A^{c/-}$ newborn died within the first month after birth, with the more severely affected mutants surviving only a few hours after delivery. In addition, $A^{c/-}$ mutant mice showed severe growth retardation and

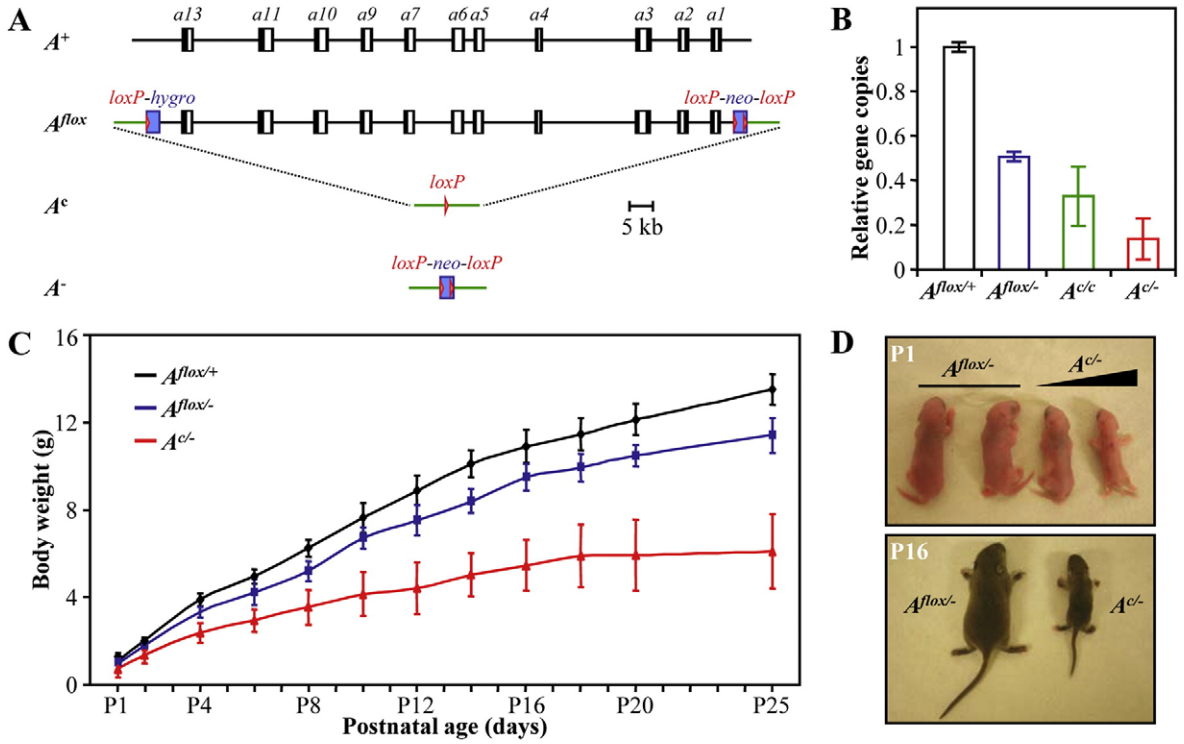

Fig. 1. Conditional deletion of the *HoxA* cluster using *T-Cre* deleter mice. (A) Schematic representation of intact (*HoxA*$^{+}$ or *A*$^{+}$), floxed (*HoxA*^{flox} or *A*^{flox}), conditionally deleted (*HoxA*^{c} or *A*^{c}) or fully deleted (*HoxA*$^{-}$ or *A*$^{-}$) *HoxA* cluster alleles used in this study. (B) Control of *T-Cre*-mediated *HoxA* cluster deletion using quantitative real-time PCR on newborn genomic DNA. Values represent the mean of more than hundred control (*A*$^{flox/+}$) and mutant (*A*$^{flox/-}$, A$^{c/c}$ and *A*$^{c/-}$) animals, after normalization to the *A*$^{flox/+}$ genotype. They reveal the heterogeneity in deletion efficiencies using the *T-Cre* line. (C) Average curves of postnatal growth in *A*$^{flox/+}$, *A*$^{flox/-}$ and *A*$^{c/-}$ mice, extracted from six different litters. Most *A*$^{c/-}$ mutant mice died within the first month after birth, whereas all *A*$^{flox/-}$ and *A*$^{c/-}$ controls survived. (D) Gross appearance of *A*$^{flox/-}$ and *A*$^{c/-}$ littermate mice at postnatal days P1 (top) and P16 (bottom). Increasing efficiency of the *T-Cre*-mediated deletion correlates with the decreasing size of newborn mice (*A*$^{c/-}$, top).

were easily distinguishable from control *A*$^{flox/+}$ and *A*$^{flox/-}$ littermates by their smaller size (Fig. 1C and D). Interestingly, the growth defect was already apparent at the perinatal stage, especially in mutant mice with high efficiency of *HoxA* recombination and became enhanced thereafter during the whole postnatal period (Fig. 1C and D). Around 2 weeks after birth, surviving *A*$^{c/-}$ mice were already two to three-fold smaller than their control littermates (Fig. 1D).

Skeletal defects

To precisely locate those cells or tissues derived from *Cre*-recombinase expressing cells, we crossed *T-Cre* transgenic mice with the *Rosa26R* (*R26R*) reporter line, which transcribes a *LacZ* allele only after *Cre*-mediated recombination has occurred (Soriano, 1999). In agreement with previous studies (Liu et al., 2003; Showell et al., 2004), β-galactosidase activity was detected in the mesoderm of developing limbs and somites, but not in neural tissues (Fig. 2A).

We determined the morphological consequences of *T-Cre*-mediated deletion of the *HoxA* cluster by comparing *A*$^{c/-}$ and *A*$^{flox/+}$ newborns skeletal preparations for both their axial and appendicular skeletal elements (Fig. 2B–D). While *A*$^{flox/+}$ control axial skeletons expectedly displayed 7 cervical, 13 thoracic, 6 lumbar and 4 sacral vertebrae (C7–T13–L6–S4), the analysis of twenty *A*$^{c/-}$ mutants newborns demonstrated mild phenotypes at both the cervico-thoracic and thoraco-lumbar transitions (Fig. 2B). The most penetrant class of *A*$^{c/-}$ mutants (10 out of 20 mice) contained additional ribs on both the last cervical and the first lumbar vertebrae, thus leading to the loss of the seventh cervical and gain of two thoracic vertebrae (C6–T15–L6–S4). In the latter mice, additional ribs were only found bilaterally (10 out of 10 mice), but cervical ribs were either fused to the costal cartilage of the first thoracic ribs (8/10 mice; Fig. 2B) or directly connected to the sternum (2/10 mice). In addition, a significant fraction of *A*$^{c/-}$ animals (8/20 mice) displayed only a transformation of the first lumbar into a 14th thoracic vertebra (with 2 out of 8 and 6 out of 8 mice showing either unilateral, or bilateral ribs, respectively). This was sometimes accompanied by a reduction in the total number of vertebrae (C7–T14–L5–S4 in 6 out of 8 mice), yet not systematically (C7–T14–L6–S4 in two specimens). Finally, the last two *A*$^{c/-}$ mutants (2/20 mice) showed a transformation of the seventh cervical vertebra into a thoracic type, directly connected to the sternum (C6–T14–L6–S4). Therefore, the overall number of sacral and caudal vertebrae remained unchanged in *A*$^{c/-}$ mutants (Fig. 2B and Supplementary Fig. 1).

A$^{c/-}$ mutant newborns had severe defects in their forelimb skeleton, in agreement with a previous study using the *Prx1-Cre* deleter strain (Kmita et al., 2005), and also in their hindlimbs (Fig. 2C and D). When compared to *A*$^{flox/+}$ controls, *A*$^{c/-}$ mutants showed a marked size reduction of their zeugopods in both forelimbs and hindlimbs. In addition, the thumbs were missing and all digits were strongly reduced in size due to the lack of some phalanges, in both *A*$^{c/-}$ mutant limbs (Fig. 2C and D). Finally, abnormal and sometimes unilateral patterns of carpal and tarsal elements were also scored with variable occurrence, in *A*$^{c/-}$ autopods (Fig. 2C and D). Altogether, the deletion of the entire *HoxA* cluster in mesodermal lineages had a rather mild morphological impact upon both the axial and the appendicular skeleton, suggesting again high functional redundancy from other *Hox* gene clusters.

Phenotypic consequences in tissues of mesodermal origin

We look for functional contributions of *Hoxa* cluster genes in a variety of organs containing a mesodermal compartment and

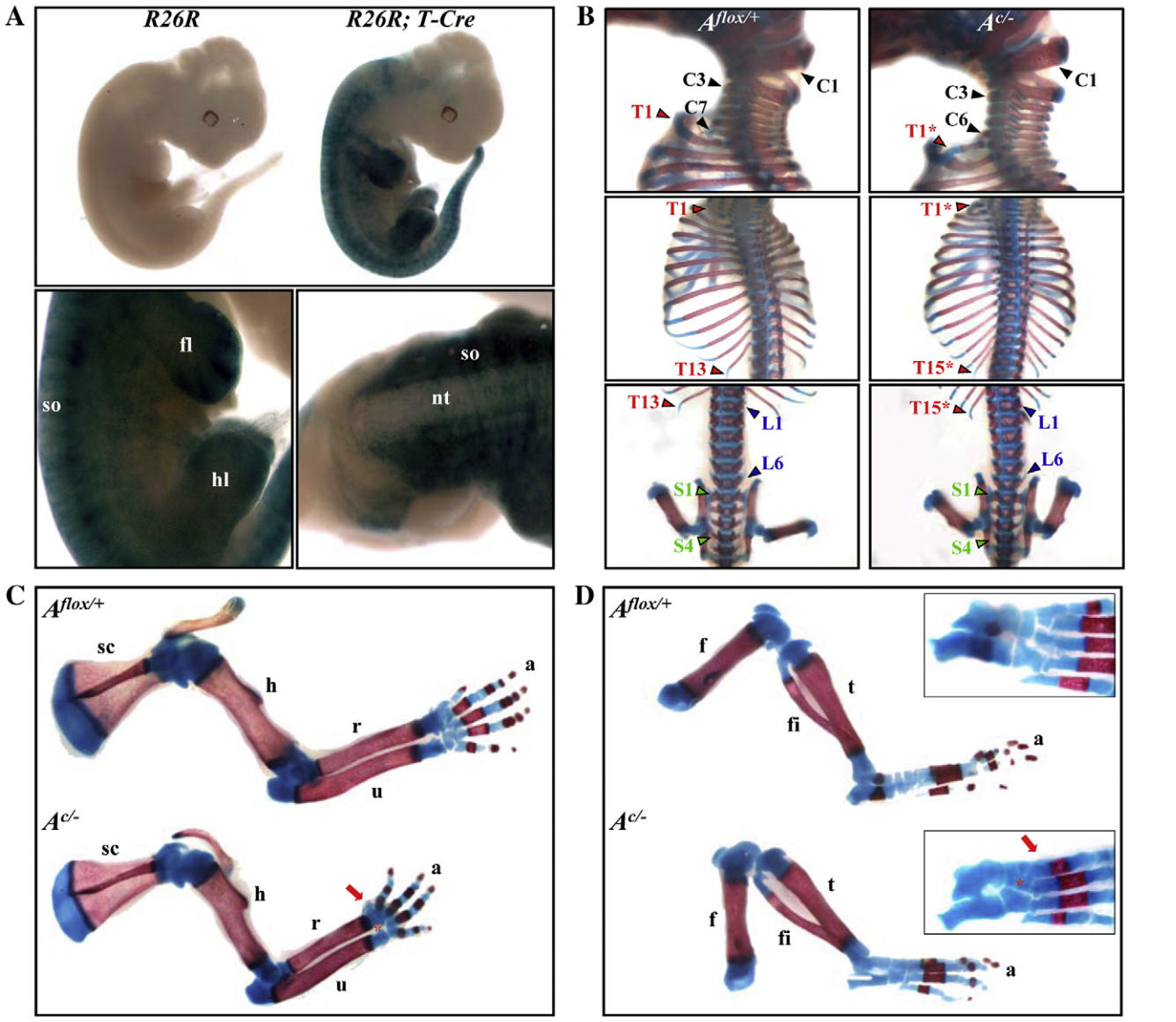

Fig. 2. Skeletal defects in *T-Cre*-mediated deletion of the *HoxA* cluster. (A) Whole-mount *LacZ* staining of E12.5 control *R26R* and *R26R*; *T-Cre* embryos (top panel). *T-Cre*-mediated activation of the *R26R* reporter allele was relatively high in somites (so), as well as in developing forelimbs (fl) and hindlimbs (hl), whereas absent from the neural tube (nt) (bottom). (B) Lateral view of the cervical region (top) as well as ventral views of thoracic (middle) and lumbo-sacral regions (bottom) from control $A^{flox/+}$ (left) and $A^{c/-}$ (right) newborn mice. The different types of vertebrae are indicated as C (cervical), T (thoracic), L (lumbar), S (sacral) or Cd (caudal), followed by a number identifying their positions in each region. Asterisks indicate additional thoracic vertebrae in $A^{c/-}$ mutants. Ribs on T1* are fused to the cartilage of the next thoracic ribs. (C and D) Newborn forelimb (C) and hindlimb (D) skeletons (blue, cartilage; red, bone). The humerus (h), radius (r), ulna (u) and tibia (t) are shortened in the $A^{c/-}$ mutant forelimb. Thumbs (arrow) as well as some carpal bones (asterisk) are missing in the $A^{c/-}$ autopod (a). f, femur; fi, fibula; sc, scapula.

performed histological sections of newborn thoracic cavities from either *R26R; T-Cre*, $A^{c/-}$ mutant or $A^{flox/+}$ control mice. The analysis of β-galactosidase reporter activity in the *R26R; T-Cre* line (Fig. 3; top) revealed a strong efficiency of *T-Cre*-mediated recombination in virtually all mesoderm-derived tissues including the lungs, the spleen, the kidneys, the gonads, as well as the adrenal glands and dorsal skin dermis (see Fig. 5B). In addition, positive β-galactosidase activity was detected within restricted areas of the developing heart, including both the endocardium and myocardium (Fig. 3).

Histological examination of newborn mice revealed a spectrum of defects in $A^{c/-}$ mutant specimen, when compared to littermate controls. First, the more severe class of $A^{c/-}$ mutants (those dying right after birth) had unusually compacted lungs, resulting from both an increase in the thickness of the alveolar walls and a decrease in diameter of alveoli and bronchioli (Fig. 3). Secondly, $A^{c/-}$ mice showed severe spleen hypoplasia, when compared to the $A^{flox/+}$ control organ (Fig. 3). Thirdly, while the mutant kidneys and gonads appeared relatively similar to control, a significant proportion of $A^{c/-}$ animals surviving birth for at least 3 weeks developed variable degrees of unilateral or bilateral polycystic kidneys (data not shown), as previously reported in animals lacking the entire *HoxD* cluster (Di-Poi et al., 2007). Finally, we noticed abnormally dilated ventricles in the developing heart and a strong reduction in the size of the thymus in $A^{c/-}$ mutants at birth, despite its mostly endodermal origin (Fig. 3 and Supplementary Fig. 2A). Other internal tissues from mutant animals, including the entire urogenital tract and organs derived from non-mesodermal germ layers, appeared grossly normal at birth (data not shown). Altogether, these results confirmed the critical role for *Hoxa* genes in the patterning of several tissues of (at least partial-) mesodermal origin, including the lungs, heart and spleen, as reported using single loss of function approaches (Aubin et al., 1997; Chisaka and Capecchi, 1991; Lawrence et al., 1997).

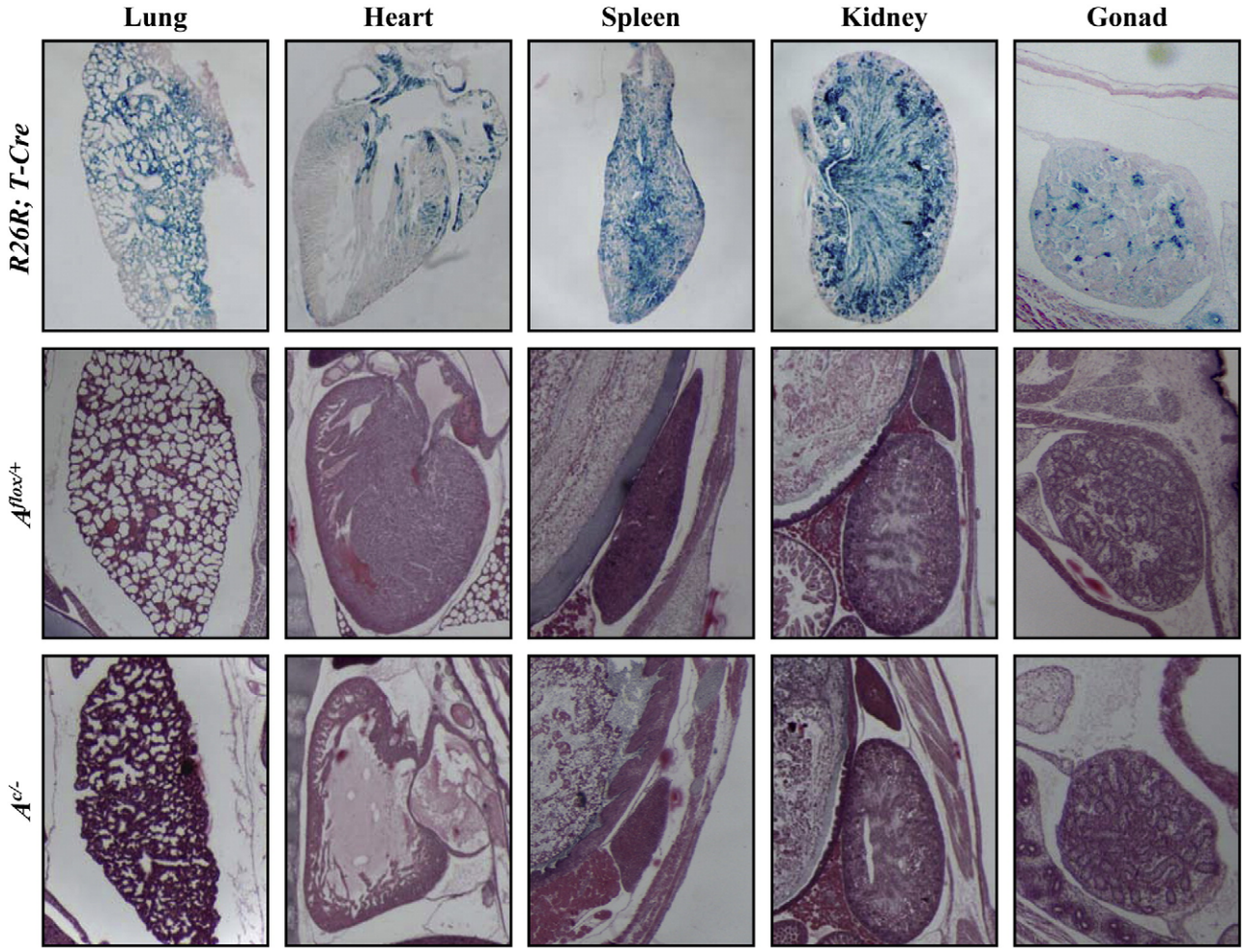

Fig. 3. Effects of *HoxA* cluster deletion on mesodermal lineages. Sagittal sections through mesoderm-derived tissues from *R26R*; *T-Cre* newborn mice stained for *LacZ*, showing the specific recombination pattern of *T-Cre* in lungs, heart, spleen, kidneys and gonads (top). Sagittal sections illustrate the abnormal development of the lungs, heart and the spleen in mutant $A^{c/-}$ (bottom) mice, when compared to controls ($A^{flox/+}$, middle).

Function of Hoxa genes during hematopoiesis

A role for *Hox* genes during hematopoiesis has been documented, yet the phenotypes reported for either single or compound mutant mice are rather mild, at least under normal conditions (McGonigle et al., 2008). This raised the question as to whether some particular *Hox* genes had been co-opted for this critical differentiation pathway or if entire gene cluster(s) would coordinately devote part of their function to this system. In this latter case, functional redundancy may once again explain the moderate severity of these phenotypes. Because of the drastic size reduction of both spleen and thymus in $HoxA^{c/-}$ mutant mice at birth (Supplementary Fig. 2A), we used fluorescence-activated cell sorter (FACS) analysis of lineage specific surface antigens to evaluate the distribution of several hematopoietic and lymphoid progenitor populations (Table 1).

The absolute cell numbers were strongly reduced within all hematopoietic compartments of $HoxA^{c/-}$ mutants, when compared to $A^{flox/+}$ age- and sex-matched controls, from three-fold in the bone marrow (BM) to five-fold in the spleen and up to eight-fold in the thymus (Fig. 4A). FACS analysis of BM, thymus and spleen cells from $A^{c/-}$ newborn mutants further demonstrated a global reduction of myeloid (granulocytes and macrophages), erythroid (erythrocytes) and lymphoid (B- and T-cells) cells, from early to mature stages of development (Table 1), albeit all lineages were generated. In addition, a subtle but consistently observed impairment of erythrocyte and thymocyte maturation, as characterized by the accumulation of immature erythrocyte and T-cell progenitors was noticed in $A^{c/-}$ newborn mutants (Fig. 4B and Supplementary Fig. 2B), as well as an increase in the percentage of KLS-HSCs (defined as $CD117^+$; Lin^-; $Sca\text{-}1^+$; Fig. 4C). Also, the relative percentage of all KLS progenitor subpopulations was increased in $A^{c/-}$ mutants at birth (Fig. 4D), pointing to an inherent defect of these progenitors to progress towards more mature lineages.

This impairment in the development of the hematopoietic system could either be the direct consequence of an important loss of function of the *HoxA* gene cluster within hematopoietic progenitor cells, or the indirect effect of the numerous alterations described above, in particular the postnatal respiratory problem, the cardiac, urogenital or skeletal defects. Therefore, we assessed whether the observed reduction in absolute cell numbers in all hematopoietic lineages was a progenitor cell-autonomous or non-autonomous effect. For this purpose, we generated fetal liver (FL) chimeras from E12.5 or E13.5 embryos. FL chimeras were established since the accumulation of the developmental defects caused premature death of the mice postnatally and thus adult BM could not be used. $CD45.2^+$ FL cells from either $HoxA^{flox/+}$ control ($n=6$) or $A^{c/-}$ mutant ($n=7$) embryos were transplanted together with $CD45.1^+$ rescue BM into lethally irradiated congenic $CD45.1^+$ recipients. While $HoxA^{flox/+}$ control cells fully reconstituted the host recipients 12 weeks post FL transplantation ($>85\%$ $CD45.2^+$ chimerism) as expected, about half (4 out of 7 mice) of $HoxA^{c/-}$ FL donor cells were able to successfully reconstitute them, with variable efficiencies (26% to 90% $CD45.2^+$ chimerism; Fig. 4E). FL

Table 1
Absolute cell numbers in different hematopoietic compartments of $A^{flox/+}$ and $A^{c/-}$ newborn mice (count $\times 10^3$).

			$A^{flox/+}$	$A^{c/-}$
Bone marrow	Immature B-cells	$CD19^+$; $B220^+$; $CD43^+$	74 ± 12	37 ± 4**
	Mature B-cells	$CD19^+$; $B220^+$; IgM^+	64 ± 17	36 ± 12**
	Immature myeloid cells	$CD11b^+$; $Gr1^+$	932 ± 401	143 ± 52**
	Granulocytes	CD11b−; $Gr1^+$	654 ± 151	283 ± 59*
	Macrophages	$CD11b^+$; $Gr1^-$	264 ± 63	207 ± 42
	Immature erythrocytes	$CD71^+$; $Ter119^-$	156 ± 57	120 ± 48
	Early erythrocytes	$CD71^+$; $Ter119^+$	2065 ± 577	908 ± 356*
	Late erythrocytes	$CD71^-$; $Ter119^+$	424 ± 106	168 ± 27**
	HSCs	$CD117^+$; Lin^-; $Sca\text{-}1^+$	7,7 ± 1,7	5,7 ± 1,0
	LT-HSCs	Lin^-; $CD34^-$; $CD135^-$	0,9 ± 0,1	0,8 ± 0,1
	ST-HSCs	Lin^-; $CD34^+$; $CD135^-$	3,3 ± 0,9	2,8 ± 0,8
	MPPs	Lin^-; $CD34^+$; $CD135^+$	3,6 ± 1,1	2,2 ± 1,0
Thymus	DN1 T-cells	Lin^-; $CD117^+$; $CD44^+$; $CD25^-$	2,2 ± 0,2	0,3 ± 0,1**
	DN2 T-cells	Lin^-; $CD117^+$; $CD44^+$; $CD25^+$	8,8 ± 1,6	1,4 ± 0,4**
	DN3 T-cells	Lin^-; $CD117^-$; $CD44^-$; $CD25^+$	20 ± 2,8	4,2 ± 1,7**
	DN4 T-cells	Lin^-; $CD117^-$; $CD44^-$; $CD25^-$	17 ± 3,9	2,8 ± 1,2**
	DP T-cells	$CD4^+$; $CD8^+$; $TCR\beta^{low/middle}$	23433 ± 4213	2576 ± 472**
	CD4SP T-cells	$CD4^+$; $CD8^-$; $TCR\beta^{high}$	2297 ± 570	207 ± 38**
	CD8SP T-cells	$CD4^-$; $CD8^+$; $TCR\beta^{high}$	405 ± 185	60 ± 25**
	γδ T-cells	$TCR\beta^-$; $TCR\gamma\delta^+$	205 ± 32	34 ± 17**
Spleen	B-cells	$B220^+$; $TCR\beta^-$	942 ± 334	284 ± 116**
	Immature myeloid cells	$CD11b^+$; $Gr\text{-}1^+$	290 ± 60	61 ± 31**
	Granulocytes	$CD11b^-$; $Gr\text{-}1^+$	383 ± 76	91 ± 34**
	Macrophages	$CD11b^+$; $Gr\text{-}1^-$	218 ± 27	143 ± 62*
	Immature erythrocytes	$CD71^+$; $Ter119^-$	382 ± 33	110 ± 33**
	Early erythrocytes	$CD71^+$; $Ter119^+$	4737 ± 808	970 ± 303**
	Late erythrocytes	$CD71^-$; $Ter119^+$	836 ± 65	107 ± 53**

cells from other $HoxA^{c/-}$ donor embryos (3 out of 7 mice) totally failed to reconstitute the host recipients, accounting for less than 1% of the $CD45.2^+$ chimeric contribution, and were thus omitted from the analysis.

Further analyses of the efficiently reconstituted hematopoietic compartment of E13.5 $HoxA^{flox/+}$ control versus $HoxA^{c/-}$ mutant FL cell recipient mice revealed a striking increase in the relative percentage of KLS-HSCs in $HoxA^{c/-}$ mutant FL cell recipients, when compared to controls (Fig. 4G). Interestingly, mutant hematopoietic progenitor cells were partially arrested at the transition from the ST-HSC (Lin^-; $CD117^+$; $Sca\text{-}1^+$; $CD34^+$; $CD135^-$) to the MPP (Lin^-; $CD117^+$; $Sca\text{-}1^+$; $CD34^+$; $CD135^+$) cell stage (Fig. 4H). Consequently, the absolute cellularity of $CD45.2^+$ mutant-derived BM cells was reduced by four-fold. This observation may account for a deficiency of $HoxA^{c/-}$ mutant FL cells to properly generate hematopoietic lineages. Chimeric recipients were thus further assessed for the efficiency of E13.5 $HoxA^{flox/+}$ control or $HoxA^{c/-}$ mutant FL cell progenitors to produce mature hematopoietic lineages. All lineages (lymphoid and myelo-granulocytic; data not shown) were generated properly with respect to relative ratios, yet the absolute cell numbers were reduced accordingly. Strikingly, the generation of mature erythrocytes was severely impaired in $HoxA^{c/-}$ mutant FL cell progenitors, particularly in the output of early erythrocytes ($CD71^+$; $Ter119^+$; Fig. 4F).

Altogether, the deletion of the entire *HoxA* cluster, analyzed in a long-term FL transplantation assay, does not influence the generation of mature lymphoid and myeloid lineages. However, mutant $HoxA^{c/-}$ FL cells inefficiently produce erythrocytes, which accounts for the obvious anemic phenotype observed in the BM and spleen. In this context, it is interesting to note that the severe impairment in generating erythrocytes was only observed in the transplantation setting (Fig. 4F) of an adult BM microenvironment using FL cells and not in $HoxA^{c/-}$ newborn mutants (Fig. 4B). These results could suggest that the function of the *HoxA* gene cluster is more important in the adult as opposed to fetal erythropoiesis. Alternatively, FL progenitors do not respond appropriately within the adult BM microenvironment and thus reflect the well known differences between embryonic and adult hematopoiesis (McGrath and Palis, 2008). In addition, immature hematopoietic progenitor cells poorly progress from the ST-HSC stage to the MPP stage. Our data thus indicate a global role for the *Hoxa* genes in the regulation of early HSCs and erythrocytic progenitors in a cell autonomous fashion.

HoxA/HoxD clusters double-mutant mice

To partially overcome the buffering effect of functional redundancy, we evaluated potential developmental defects in the absence of both *HoxA* and *HoxD* clusters, an approach that had previously unmasked functional aspects of these genes in early limb buds (Kmita et al., 2005; Tarchini et al., 2006). We engineered combined deletions of *Hoxa* and *Hoxd* genes, using the conditional allele of the *HoxA* cluster ($A^{c/-}$) together with various targeted deletions within the *HoxD* cluster. Double-mutant embryos harboring a conditional deletion of *Hoxa* genes with *T-Cre* ($A^{c/-;T}$), combined either with the absence of all *Hoxd* genes (referred to as $A^{c/-;T}$; $D^{d(1-13/d(1-13)}$), or with the deletion of the *Hoxd13* to *Hoxd4* interval ($A^{c/-;T}$; $D^{d(4-13/d(4-13)}$), died *in utero* before embryonic day 11.5. Consequently, we used a shorter deletion within the *HoxD* cluster, by re-introducing posterior *Hoxd13* and *Hoxd12* gene functions to the latter deletion ($A^{c/-;T}$; $D^{d(4-11)/d(4-11)}$).

($A^{c/-;T}$; $D^{d(4-11)/d(4-11)}$) double-mutant fetuses died between E15.5 and E16.5. They displayed skin edema and a significant reduction of approximately one third in the number of caudal vertebrae when compared to $A^{+/+}$; $D^{+/+}$ controls (Fig. 5A), two phenotypes likely produced by distinct mechanisms. The skin alterations were indeed also noticed in a few embryos heterozygous for a full *HoxD* deletion and the conditional *HoxA* allele ($A^{c/-;T}$; $D^{d(1-13)/+}$), indicating that this novel phenotype was induced by the combined loss of functions of both *Hoxa* and *Hoxd* genes lying within the *Hoxd11* to *Hoxd4* interval. Histological analysis of double-mutant $A^{c/-;T}$; $D^{d(4-11)/d(4-11)}$ edematous skin revealed a remarkable absence (or delay) of epidermal stratification and epithelial appendage differentiation, in relation with a strong efficiency of *T-Cre*-mediated recombination in skin dermal fibroblasts (Fig. 5B). In contrast, the defect in axial elongation was only observed in $A^{c/-;T}$; $D^{d(4-11)/d(4-11)}$ double-mutants, indicating that this

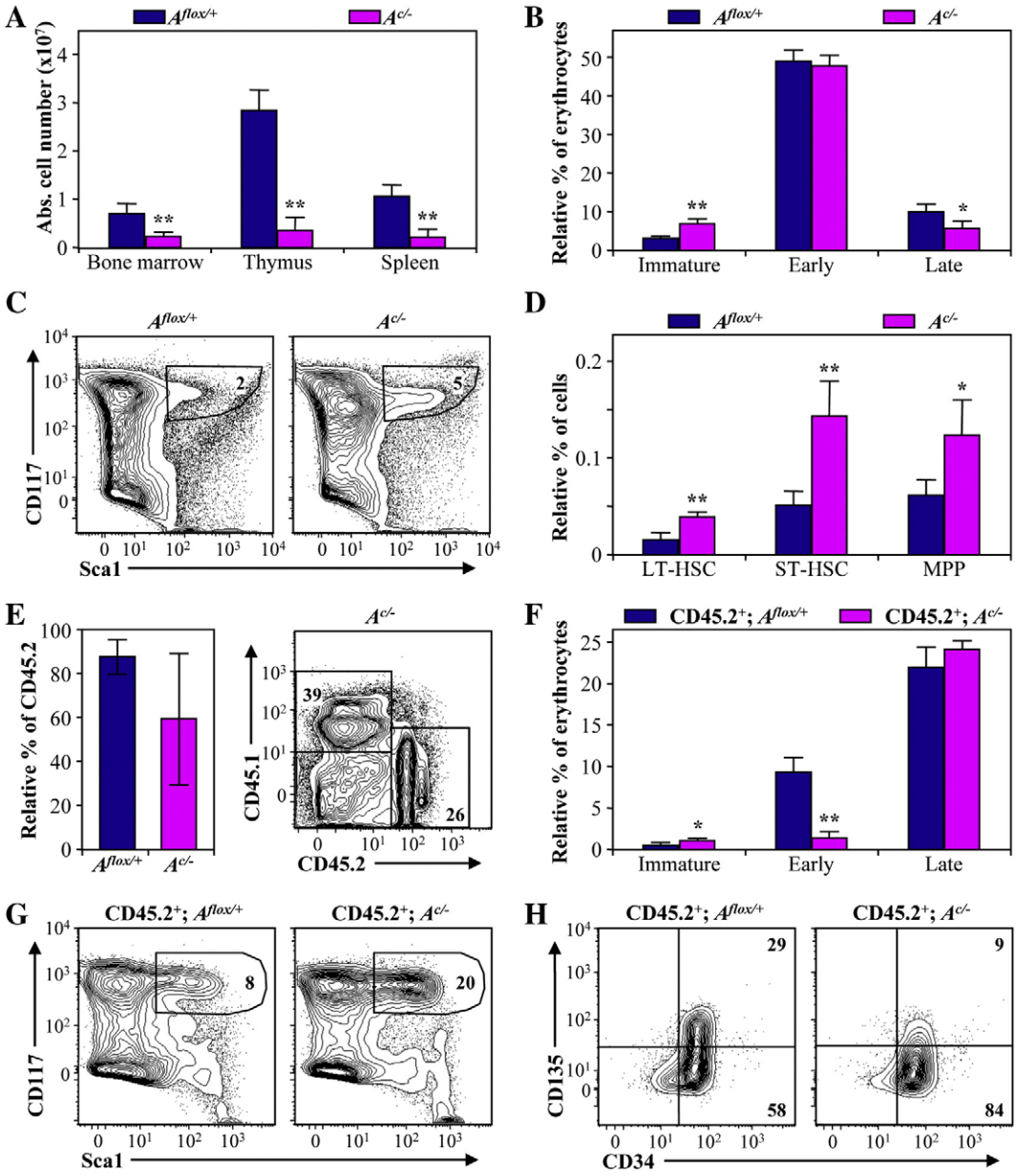

Fig. 4. Hematopoietic defects in *HoxA*$^{c/-}$ mutant mice. (A) Absolute numbers of cells from bone marrow (BM), thymus and spleen in $A^{flox/+}$ and $A^{c/-}$ newborn mice. Values are mean percentages of total cells in at least four animals per genotype. (B) Relative percentages of the erythrocytic lineage of BM cells from $A^{flox/+}$ (left) and $A^{c/-}$ (right) newborn mice: immature erythrocytes (CD71$^+$; Ter119$^-$); early erythrocytes (CD71$^+$; Ter119$^+$); late erythrocytes (CD71$^-$; Ter119$^+$). Four independent analyses have been performed per genotype. (C and D) Representative flow cytometric analysis of KLS-HSCs (defined as CD117$^+$; Lin$^-$; Sca-1$^+$) and absolute relative percentages of KLS-HSC subpopulations LT-HSC (CD34$^-$; CD135$^-$), ST-HSC (CD34$^+$; CD135$^-$) and MPP (CD34$^+$; CD135$^+$), after gating on Lin$^-$ BM cells derived from $A^{flox/+}$ and $A^{c/-}$ newborn mice. (E–H) Long-term fetal liver (FL) transplants of E13.5 *HoxA*$^{flox/+}$ and *HoxA*$^{c/-}$ mutant embryos. Relative percentages of CD45.2$^+$ contribution of FL-derived progeny from *HoxA*$^{flox/+}$ and *HoxA*$^{c/-}$ reconstituted chimeric mice 12 weeks post FL transplantation (E, left panel), and representative flow cytometric analysis of *HoxA*$^{c/-}$ with low reconstitution efficiency after long-term transplantation (E, right panel, 7 months). Relative percentages of the erythroid lineage in *HoxA*$^{flox/+}$ and *HoxA*$^{c/-}$ FL cell reconstituted chimeras (F). Representative flow cytometric analysis of KLS-HSCs after gating on Lin$^-$ BM cells derived from $A^{flox/+}$ and $A^{c/-}$ reconstituted recipient mice (G), and further analysis of KLS-HSC subpopulations LT-HSC, ST-HSC and MPP defined by expression of CD34 and CD135 surface antigens as indicated above (H). Independent Student's *t*-test: $^*P<0.05$; $^{**}P<0.01$.

phenotype was rather derived from a mis-regulation of remaining *Hoxd* genes.

We tried to overcome the early lethality of the double *HoxA*/*HoxD* clusters deletion, and hence to see its effect upon axial extension and patterning, by using the mesoderm-specific elements of the *Delta1* (*Dll1*) gene. We used this promoter to conditionally delete the *HoxA* cluster ($A^{c/-;Dll1}$) within the presomitic mesoderm (PSM) and structures derived thereof (Beckers et al., 2000), in combination with the absence of the *HoxD* cluster ($A^{c/-;Dll1}$; $D^{d(1-13/d(1-13)}$). Double mutant embryos were smaller than their littermates, yet they survived throughout embryonic development, allowing us to carry out whole skeletal preparations. $A^{c/-;Dll1}$; $D^{d(1-13/1-13)}$ exhibited surprisingly minor skeletal defects, mainly reminiscent of phenotypes caused either by deleting the *HoxA* (for example the loss of the seventh cervical and gain of two thoracic vertebrae) or the *HoxD* cluster (for example the posteriorization of the lumbo-sacral transition, with seven or eight lumbar vertebrae instead of six; Zakany et al. 2001). In addition, we observed a strong reduction of the first cervical vertebra or atlas (Fig. 5C), most probably due to the combined deletion of *Hoxa3* and *Hoxd3* genes (Condie and Capecchi, 1994). This phenotype precluded the observation of what had been reported for *Hoxa4*/*Hoxd4* double mutant mice, where the atlas was fused to the axis.

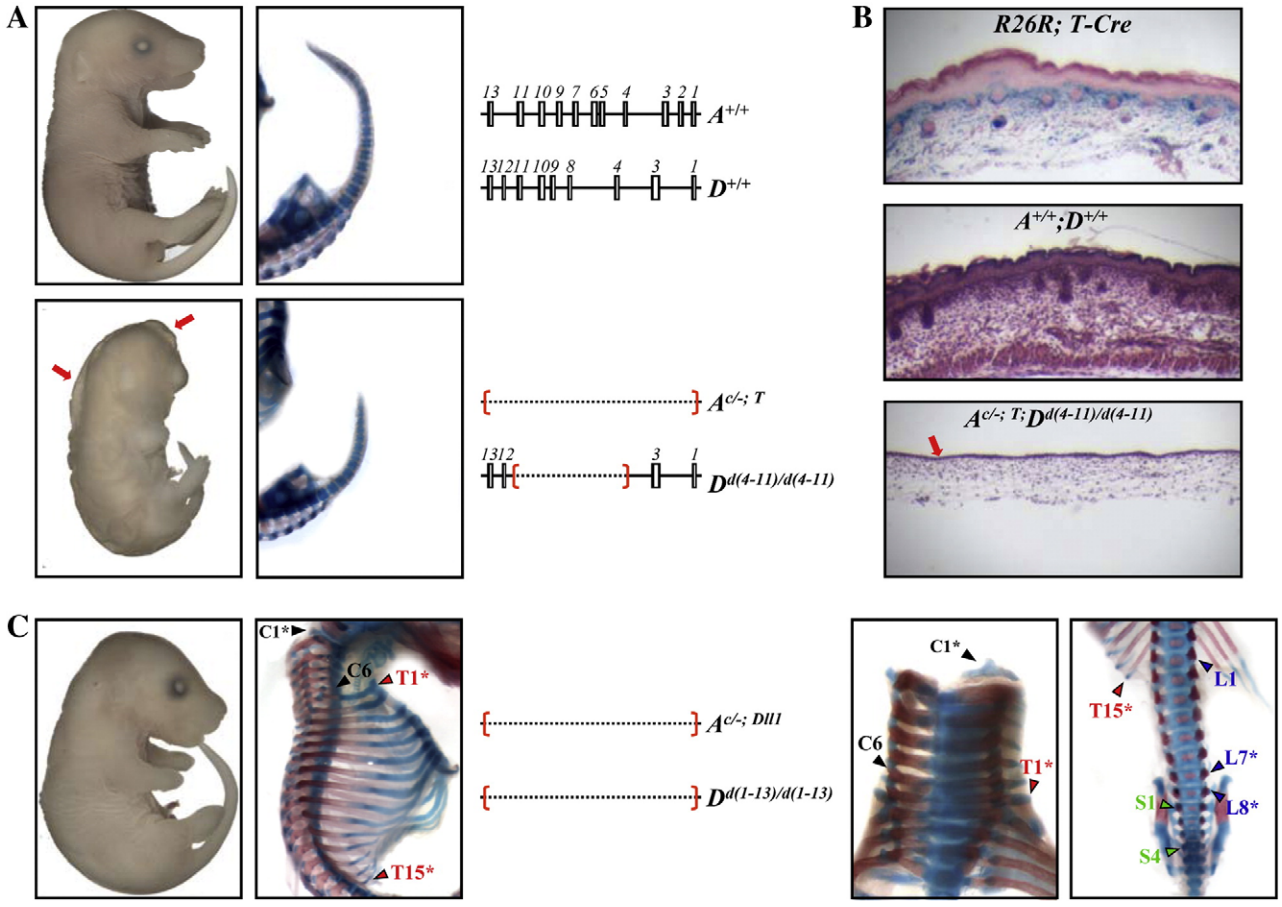

Fig. 5. *HoxA*/*HoxD* double-mutant embryos using *T-Cre* and *Dll1-Cre* transgenic mice. (A) Sagittal views of wild type ($A^{+/+}$; D^{++}) and double-mutant ($A^{c/-;T}$; $D^{d(4-11)/d(4-11)}$) embryos (left) and caudal axial skeleton (middle) at embryonic day E16.5. Note the embryonic skin edema (arrows) and shorter tail in the double-mutant expressing *T-Cre*. Genotypes are indicated (right). (B) Sagittal sections of *LacZ*-stained *R26R*; *T-Cre*, showing the specific recombination pattern of *T-Cre* in the dermal layer (top) and a stained $A^{+/+}$; D^{++} and $A^{c/-;T}$; $D^{d(4-11)/d(4-11)}$ dorsal skin, with the abnormally thin epidermal layer in the double-mutant embryo at E16.5 (arrow, bottom). (C) Sagittal views of double-mutant ($A^{c/-;Dll1}$; $D^{d(1-13)/d(1-13)}$) embryo and anterior axial skeleton (left panels) at embryonic day E16.5. High magnifications of cervical and lumbo-sacral regions from double mutant skeletons are shown in the right panels. Note the severe reduction of the atlas (C1*) as well as the addition of two thoracic (T1* and T15*) and two lumbar (L7* and L8*) vertebrae in the double-mutant expressing *Dll1-Cre*.

Discussion

Deletion of entire *Hox* gene clusters is an essential step towards a full understanding of the functional coherence of this gene family. This level of understanding has been made arguably difficult, due to the functional redundancy of the system, generated by the shared evolutionary histories of these gene clusters. On the one hand, the two rounds of genome duplications produced—a maximum of four—paralogous genes, and hence a large functional overlap for those functions potentially present in ancestral animals. This is well illustrated by the effect of combining inactivations of paralogous *Hox* genes upon axial patterning (e.g. Wellik and Capecchi, 2003). On the other hand, the existence of gene clusters triggered the emergence of global and coordinated regulations involving several genes in *cis* (Duboule, 2007), thus leading to functional redundancy between neighboring, rather than paralogous genes. Consequently, full cluster deletions may reveal the existence of *Hox* cluster-specific functions, generally associated with the emergence of vertebrates, i.e. that evolved after cluster duplications. The coordinated functions of either *Hoxd* genes in kidneys (Di-Poi et al., 2007) or *Hoxa* genes in crest cells (Minoux et al., 2009) illustrate this phenomenon.

A lethal condition

Such large compound deletions, involving 11 genes altogether (for *HoxA*) understandably lead to highly deleterious conditions. Mice lacking all *Hoxa* gene functions in mesodermal lineages indeed suffered from a spectrum of abnormalities, including respiratory, cardiac and hematopoietic defects, which prevented mutant animals to reach postnatal development, at least for those with a high level of *Cre*-induced recombination. Individual loss-of-function mutations were previously generated for several *Hoxa* genes expressed in the respiratory tract, yet only the loss of *Hoxa5* severely perturbed lungs development and maturation, resulting in respiratory defects and high rates of perinatal lethality (Aubin et al., 1997). Likewise, the *Hoxa3* mutation induced markedly reduced postnatal viability, due to multiple defects in organogenesis, including the agenesis of the thymus and parathyroid glands, a hypoplasia of the thyroid gland as well as alterations in both the heart and arteries (Chisaka and Capecchi, 1991). Therefore, the perinatal lethality observed in our more severe class of conditional *HoxA* mutants likely resulted from strong defects in lung and heart morphogenesis, as elicited by the combined loss of functions of both *Hoxa5* and *Hoxa3*.

Likewise, those *HoxA* cluster mutant mice, which survived after birth developed different degrees of malformed polycystic kidneys, as previously reported in homeobox-swap experiments using a chimeric *Hoxa11* allele with the *Hoxa4* homeobox (Zhao and Potter, 2002). Finally, a reduced fertility was noticed in *HoxA* mutant females, resulting from the defective early uterine environment reported when *Hoxa10* or *Hoxa11* were removed in isolation (Benson et al., 1996; Hsieh-Li et al., 1995).

Defects in skeletal patterning and axial elongation

As for all *Hox* clusters, *Hoxa* genes are strongly expressed in paraxial mesoderm derivatives, following the rule of collinearity (Gaunt et al., 1988). Transcription is already well established in PSM and the genes remain expressed once they establish their appropriate boundaries in somites and their derivatives. The effects of *Hox* gene mutations upon axial patterning have been largely described and typically impact upon the number and type of vertebrae in specific regions of the axial skeleton. For instance, members of *Hox4*, *Hox5* and *Hox6* paralogous groups regulate the number and identity of cervical and thoracic vertebrae, members of *Hox9* and *Hox10* group regulate thoracic and lumbar identity, whereas *Hox11* genes specify the sacral region.

HoxA cluster conditional mutant mice showed series of axial phenotypes, which can be interpreted as the addition of single gene functions. As such, these mice exhibited an ectopic rib formation on the last cervical vertebra, similar to the effect of knocking out *Hoxa4*, *Hoxa5* or *Hoxa6*, as well as on the first lumbar vertebra, similar to what follows the abrogation of either *Hoxa9* or *Hoxa10* (Favier et al., 1996; Fromental-Ramain et al., 1996a; Jeannotte et al., 1993; Kostic and Capecchi, 1994). Altogether, the defects observed in the axial skeleton were rather mild, comparable to what was observed upon deletion of either the *HoxB*, *HoxC* or *HoxD* clusters (Medina-Martinez et al., 2000; Suemori and Noguchi, 2000; Zakany et al., 2001), suggesting that *HoxB*, *HoxC* and/or *HoxD* cluster genes largely compensated for the effect of this conditional deletion on AP skeletal patterning.

The axial skeleton is arguably one of the structures where functional redundancy between *HOX* products is the most remarkable (e.g. Wellik and Capecchi, 2003). We tried to address this issue by deleting the full *HoxD* cluster, on the top of the mesoderm-conditional *HoxA*, but double mutant embryos never reached E11.5. The same problem was encountered when using a shorter deletion within *HoxD*, removing from *Hoxd4* to *Hoxd13* included. We then used another *Cre*-deleter strain that is active in the PSM exclusively and obtained newborns lacking both the *HoxD* cluster and the *HoxA*, presumably in derivatives of the PSM. Here again, the phenotypes were mild, yet the clear effect upon the cervical vertebrae (i.e. the expected absence of atlas due to lack of *Hoxa3* and *Hoxd3*; Condie and Capecchi, 1994) indicated a fair level of conditional deletion. This result suggests that the vertebral column can be globally patterned, though with some minor alterations, by only two gene clusters, among which one lacking all 'posterior' genes but group 13 (*HoxB*; Economides et al., 2003).

To combine with the conditional *HoxA* allele, we also used one deletion within *HoxD*, leaving in place both the most anterior and most posterior *Hoxd* genes. Double mutant fetuses developed substantially better that other combined configurations involving the *T* deleter strain. Interestingly, 5 out of 10 double mutant embryos displayed a significantly shorter tail. We explain this defect by a gain of function of the remaining posterior *Hoxd* genes (*Hoxd13* and/or *Hoxd12*), whose function may be to terminate axial elongation, perhaps by antagonizing the functions of more anterior *Hox* genes, as reported previously during the development of limbs and kidneys (Di-Poi et al., 2007; Kmita et al., 2002). Recent experiments involving transgenic gains of function of group 13 genes have also lead to important truncations of the posterior trunk (Young et al., 2009), in agreement with the loss of function of *Hoxb13*, which tend to slightly elongate the tail (Economides et al., 2003). Noteworthy, the posterior *Hox* gene gain of function resulting from the deletion of the *Hoxd4* to *Hoxd11* interval did not elicit the same phenotype in an otherwise wild type condition, suggesting that its deleterious effect is counterbalanced by the numerous doses of genes participating to tail elongation. However, in the absence of some of these genes (the combined *HoxA* deletion), the gain of function effect is unmasked. This dosage effect is likely reduced in the transgenic approach, where more truncations are observed (Young et al., 2009).

Defect in skin morphogenesis

HoxA mutant fetuses combined with a targeted deletion within the *HoxD* cluster exhibited a striking phenotype in early skin morphogenesis, not yet scored for any *Hox* mutants. Such specimen had a largely edematous skin, without epidermal stratification and differentiation of epithelial appendages. Because *T-Cre*-mediated recombination in skin takes place in dermal fibroblasts, a novel function for *Hox* genes is proposed during the regulation of epithelial–mesenchymal interactions occurring between the epidermis and the dermis.

Interestingly, this phenotype was not observed in single *HoxA* deletion mutants and at least two of the *Hoxd* genes (*Hoxd9* and *Hoxd11*) additionally deleted in the combined mutant version, were described as being expressed in the basal layer of the epidermis (as well as in the hair matrix; Kanzler et al., 1994; Stelnicki et al., 1998), rather than in the dermis, where expression seems to resume at later stages (Reid and Gaunt, 2002). It is thus possible that the deletions of the two clusters do not affect one and the same cellular population, at the same time, and that the combined effect of these deletions reveals a function that requires the integrity of both the epidermis and dermis, for example to ensure proper induction of the former by the latter. We think that this function is distinct from that reported for *Hoxc13* during the growth of hair follicles (Godwin and Capecchi, 1998). A comparison between conditional *Hox* mutants in both epidermal and dermal compartments of the embryonic skin will be necessary to clarify the exact respective functions of different *Hox* clusters during proper epithelial differentiation, and to confirm that the skin defect observed in *HoxA*/*HoxD* double-mutants is not secondary to another phenotypic effect.

Hoxa genes in hematopoiesis

Hematopoietic cells from both mouse and human bone marrow express many *Hox* genes belonging to either the *HoxA*, *HoxB* or *HoxC* clusters, predominantly in HSC-enriched subpopulations and immature hematopoietic progenitor compartments (Argiropoulos and Humphries, 2007), suggesting important functional contributions of *Hox* genes during early hematopoiesis. While the over-expression of several *Hox* genes, including *Hoxa4*, *Hoxa9*, *Hoxa10*, *Hoxb4* and *Hoxb6*, perturbs both myeloid and lymphoid differentiation, as well as HSC proliferation *in vitro* and *in vivo* (Iacovino et al., 2009; Sauvageau et al., 1995; Thorsteinsdottir et al., 1997, 2002), only subtle defects in hematopoiesis were reported under more physiological conditions, in mice lacking single or multiple *Hox* gene functions. This includes gene members of the *HoxA* (*Hoxa5*, *Hoxa7*, *Hoxa9* and *Hoxa10*) and *HoxB* (*Hoxb4*, *Hoxb6*) clusters (Argiropoulos and Humphries, 2007; Lawrence et al., 1996).

Mice lacking the *Hoxa9* function, a gene that is highly expressed in hematopoietic cells, primarily within the HSC compartment, display the most severe hematopoietic phenotype scored for a single *Hox* gene deletion to date, including a rather modest reduction in spleen size and a decrease in cell number affecting both myeloid and lymphoid compartments (Lawrence et al., 1997). Also, *Hoxa9* mutants have severe problems during fetal thymic development, including a reduction of immature thymocytes, due to increased cell death (Izon et al., 1998). However, and despite the defective ability of *Hoxa9* mutant HSCs to repopulate irradiated recipients in competitive transplantation assays (Lawrence et al., 2005), both the numbers and frequencies of KLS-HSCs and MPPs were normal in *Hoxa9* mutant mice (Lawrence et al., 1997; Magnusson et al., 2007a; So et al., 2004).

Our conditional deletion of the entire *HoxA* cluster induced a much more dramatic phenotype than the single *Hoxa9* loss of function, in all erythroid, myeloid and lymphoid lineages, from early progenitors to more committed cells. This indicates that multiple *Hoxa* genes, rather than *Hoxa9* alone, functionally cooperate in the hematopoietic system under normal conditions. *Hoxa5*, but also probably *Hoxa10* and *Hoxa9*, might regulate the shift toward myeloid or erythroid differentiation in

human cells (Crooks et al., 1999; Ferrell et al., 2005). The loss of these three genes in *cis* may thus explain the deficiency in the proper generation of the erythrocytic lineage in our *HoxA* mutants.

Consistent with the existence of a complex network of genetic interactions between *Hox* genes in primitive hematopoiesis, deletion of the entire *HoxA* cluster, but not of *HoxB* (Bijl et al., 2006), led to defects in the early postnatal KLS-HSC compartment. In particular, the block at the ST-HSC stage demonstrates a role for several *Hoxa* genes in the maintenance and differentiation of HSCs before they adopt a myeloid, erythroid or lymphoid cell fate. *Hoxa* genes such as *Hoxa5*, *Hoxa9* and *Hoxa10*, which have been proposed to regulate HSC self-renewal, based on competitive transplantation and over-expression assays, might be necessary for the regulation of HSCs under normal conditions (Lawrence et al., 2005; Magnusson et al., 2007b; Sauvageau et al., 2004).

Recent reports have also highlighted the importance of multiple *Hox* genes in leukemic transformation. In particular, several members of the *HoxA* cluster, including *Hoxa6*, *Hoxa9*, *Hoxa10* and *Hoxa13*, are highly expressed in patients with acute myeloid or lymphoid leukemia and the mis-regulation of these genes has been associated with different models of both murine and human leukemia (Argiropoulos and Humphries, 2007; Dickson et al., 2009; McGonigle et al., 2008). The application of more refined conditional mutations whereby the *HoxA* cluster be deleted from a targeted hematopoietic tissue, for example within HSCs, will help elucidate the role of these genes into this important cell lineage.

Acknowledgments

We thank A. Gossler for the deleter strains, Nadine Fraudeau, Thi Hanh Nguyen Huynh, Fabienne Chabaud and Bénédicte Mascrez for their assistance and help with mice, as well as members of the Duboule laboratories for discussions and reagents. This work was supported by funds from the University of Geneva, the Ecole Polytechnique Fédérale, Lausanne, the Swiss National Research Fund, the National Research Center (NCCR) '*Frontiers in Genetics*', the EU program 'Crescendo' and the European Research Council (ERC).

Appendix A. Supplementary data

Supplementary data associated with this article can be found, in the online version, at doi:10.1016/j.ydbio.2010.03.006.

References

Argiropoulos, B., Humphries, R.K., 2007. Hox genes in hematopoiesis and leukemogenesis. Oncogene 26, 6766–6776.
Aubin, J., Lemieux, M., Tremblay, M., Berard, J., Jeannotte, L., 1997. Early postnatal lethality in Hoxa-5 mutant mice is attributable to respiratory tract defects. Dev. Biol. 192, 432–445.
Beckers, J., Caron, A., Hrabé de Angelis, M., Hans, S., Campos-Ortega, J.A., Gossler, A., 2000. Distinct regulatory elements direct delta1 expression in the nervous system and paraxial mesoderm of transgenic mice. Mech. Dev. 95, 23–34.
Benson, G.V., Lim, H., Paria, B.C., Satokata, I., Dey, S.K., Maas, R.L., 1996. Mechanisms of reduced fertility in Hoxa-10 mutant mice: uterine homeosis and loss of maternal Hoxa-10 expression. Development 122, 2687–2696.
Bijl, J., Thompson, A., Ramirez-Solis, R., Krosl, J., Grier, D.G., Lawrence, H.J., Sauvageau, G., 2006. Analysis of HSC activity and compensatory Hox gene expression profile in Hoxb cluster mutant fetal liver cells. Blood 108, 116–122.
Chisaka, O., Capecchi, M.R., 1991. Regionally restricted developmental defects resulting from targeted disruption of the mouse homeobox gene hox-1.5. Nature 350, 473–479.
Clements, D., Taylor, H.C., Herrmann, B.G., Stott, D., 1996. Distinct regulatory control of the Brachyury gene in axial and non-axial mesoderm suggests separation of mesoderm lineages early in mouse gastrulation. Mech. Dev. 56, 139–149.
Condie, B.G., Capecchi, M.R., 1994. Mice with targeted disruptions in the paralogous genes hoxa-3 and hoxd-3 reveal synergistic interactions. Nature 370, 304–307.
Crooks, G.M., Fuller, J., Petersen, D., Izadi, P., Malik, P., Pattengale, P.K., Kohn, D.B., Gasson, J.C., 1999. Constitutive HOXA5 expression inhibits erythropoiesis and increases myelopoiesis from human hematopoietic progenitors. Blood 94, 519–528.
Davis, A.P., Capecchi, M.R., 1996. A mutational analysis of the 5′ HoxD genes: dissection of genetic interactions during limb development in the mouse. Development 122, 1175–1185.
de la Cruz, C.C., Der-Avakian, A., Spyropoulos, D.D., Tieu, D.D., Carpenter, E.M., 1999. Targeted disruption of Hoxd9 and Hoxd10 alters locomotor behavior, vertebral identity, and peripheral nervous system development. Dev. Biol. 216, 595–610.
Deschamps, J., van den, A.E., Forlani, S., de Graaff, W., Oosterveen, T., Roelen, B., Roelfsema, J., 1999. Initiation, establishment and maintenance of Hox gene expression patterns in the mouse. Int. J. Dev. Biol. 43, 635–650.
Di-Poi, N., Zakany, J., Duboule, D., 2007. Distinct roles and regulations for HoxD genes in metanephric kidney development. PLoS. Genet. 3, e232.
Dickson, G.J., Kwasniewska, A., Mills, K.I., Lappin, T.R., Thompson, A., 2009. Hoxa6 potentiates short-term hemopoietic cell proliferation and extended self-renewal. Exp. Hematol. 37, 322–333.
Duboule, D., Dolle, P., 1989. The structural and functional organization of the murine HOX gene family resembles that of Drosophila homeotic genes. EMBO J. 8, 1497–1505.
Duboule, D., 2007. The rise and fall of Hox gene clusters. Development 134, 2549–2560.
Economides, K.D., Zeltser, L., Capecchi, M.R., 2003. Hoxb13 mutations cause overgrowth of caudal spinal cord and tail vertebrae. Dev. Biol. 256, 317–330.
Favier, B., Rijli, F.M., Fromental-Ramain, C., Fraulob, V., Chambon, P., Dolle, P., 1996. Functional cooperation between the non-paralogous genes Hoxa-10 and Hoxd-11 in the developing forelimb and axial skeleton. Development 122, 449–460.
Ferrell, C.M., Dorsam, S.T., Ohta, H., Humphries, R.K., Derynck, M.K., Haqq, C., Largman, C., Lawrence, H.J., 2005. Activation of stem-cell specific genes by HOXA9 and HOXA10 homeodomain proteins in CD34+ human cord blood cells. Stem Cells 23, 644–655.
Fromental-Ramain, C., Warot, X., Lakkaraju, S., Favier, B., Haack, H., Birling, C., Dierich, A., Dolle, P., Chambon, P., 1996a. Specific and redundant functions of the paralogous Hoxa-9 and Hoxd-9 genes in forelimb and axial skeleton patterning. Development 122, 461–472.
Fromental-Ramain, C., Warot, X., Messadecq, N., LeMeur, M., Dolle, P., Chambon, P., 1996b. Hoxa-13 and Hoxd-13 play a crucial role in the patterning of the limb autopod. Development 122, 2997–3011.
Gaunt, S.J., Sharpe, P.T., Duboule, D., 1988. Spatially restricted domains of homeo-gene transcripts in mouse embryos—relation to a segmented body plan. Development (Suppl.) 104, 169–179.
Godwin, A.R., Capecchi, M.R., 1998. Hoxc13 mutant mice lack external hair. Genes Dev. 12, 11–20.
Graham, A., Papalopulu, N., Krumlauf, R., 1989. The murine and Drosophila homeobox gene complexes have common features of organization and expression. Cell 57, 367–378.
Hsieh-Li, H.M., Witte, D.P., Weinstein, M., Branford, W., Li, H., Small, K., Potter, S.S., 1995. Hoxa 11 structure, extensive antisense transcription, and function in male and female fertility. Development 121, 1373–1385.
Iacovino, M., Hernandez, C., Xu, Z., Bajwa, G., Prather, M., Kyba, M., 2009. A conserved role for Hox paralog group 4 in regulation of hematopoietic progenitors. Stem Cells Dev. 18, 783–792.
Izon, D.J., Rozenfeld, S., Fong, S.T., Komuves, L., Largman, C., Lawrence, H.J., 1998. Loss of function of the homeobox gene Hoxa-9 perturbs early T-cell development and induces apoptosis in primitive thymocytes. Blood 92, 383–393.
Jeannotte, L., Lemieux, M., Charron, J., Poirier, F., Robertson, E.J., 1993. Specification of axial identity in the mouse: role of the Hoxa-5 (Hox1.3) gene. Genes Dev. 7, 2085–2096.
Kanzler, B., Vialler, J.P., Le Mouellic, H., Boncinelli, E., Duboule, D., Dhouailly, D., 1994. Differential expression of two different homeobox gene families during mouse tegument morphogenesis. Int. J. Dev Biol. 38, 633–640.
Kmita, M., Fraudeau, N., Herault, Y., Duboule, D., 2002. Serial deletions and duplications suggest a mechanism for the collinearity of Hoxd genes in limbs. Nature 420, 145–150.
Kmita, M., Tarchini, B., Zakany, J., Logan, M., Tabin, C.J., Duboule, D., 2005. Early developmental arrest of mammalian limbs lacking HoxA/HoxD gene function. Nature 435, 1113–1116.
Kostic, D., Capecchi, M.R., 1994. Targeted disruptions of the murine Hoxa-4 and Hoxa-6 genes result in homeotic transformations of components of the vertebral column. Mech. Dev. 46, 231–247.
Lawrence, H.J., Sauvageau, G., Humphries, R.K., Largman, C., 1996. The role of HOX homeobox genes in normal and leukemic hematopoiesis. Stem Cells 14, 281–291.
Lawrence, H.J., Helgason, C.D., Sauvageau, G., Fong, S., Izon, D.J., Humphries, R.K., Largman, C., 1997. Mice bearing a targeted interruption of the homeobox gene HOXA9 have defects in myeloid, erythroid, and lymphoid hematopoiesis. Blood 89, 1922–1930.
Lawrence, H.J., Christensen, J., Fong, S., Hu, Y.L., Weissman, I., Sauvageau, G., Humphries, R.K., Largman, C., 2005. Loss of expression of the Hoxa-9 homeobox gene impairs the proliferation and repopulating ability of hematopoietic stem cells. Blood 106, 3988–3994.
Liu, C., Nakamura, E., Knezevic, V., Hunter, S., Thompson, K., Mackem, S., 2003. A role for the mesenchymal T-box gene Brachyury in AER formation during limb development. Development 130, 1327–1337.
Magnusson, M., Brun, A.C., Lawrence, H.J., Karlsson, S., 2007a. Hoxa9/hoxb3/hoxb4 compound null mice display severe hematopoietic defects. Exp. Hematol. 35, 1421–1428.
Magnusson, M., Brun, A.C., Miyake, N., Larsson, J., Ehinger, M., Bjornsson, J.M., Wutz, A., Sigvardsson, M., Karlsson, S., 2007b. HOXA10 is a critical regulator for hematopoietic stem cells and erythroid/megakaryocyte development. Blood 109, 3687–3696.
McGinnis, W., Krumlauf, R., 1992. Homeobox genes and axial patterning. Cell 68, 283–302.
McGonigle, G.J., Lappin, T.R., Thompson, A., 2008. Grappling with the HOX network in hematopoiesis and leukemia. Front Biosci. 13, 4297–4308.
McGrath, K., Palis, J., 2008. Ontogeny of erythropoiesis in the mammalian embryo. Curr. Top. Dev. Biol. 82, 1–22.

McIntyre, D.C., Rakshit, S., Yallowitz, A.R., Loken, L., Jeannotte, L., Capecchi, M.R., Wellik, D.M., 2007. Hox patterning of the vertebrate rib cage. Development 134, 2981–2989.
Medina-Martinez, O., Bradley, A., Ramirez-Solis, R., 2000. A large targeted deletion of Hoxb1-Hoxb9 produces a series of single-segment anterior homeotic transformations. Dev. Biol. 222, 71–83.
Minoux, M., Antonarakis, G.S., Kmita, M., Duboule, D., Rijli, F.M., 2009. Rostal and caudal pharyngeal arches share a common neural crest ground pattern. Development 136, 637–645.
Perantoni, A.O., Timofeeva, O., Naillat, F., Richman, C., Pajni-Underwood, S., Wilson, C., Vainio, S., Dove, L.F., Lewandoski, M., 2005. Inactivation of FGF8 in early mesoderm reveals an essential role in kidney development. Development 132, 3859–3871.
Reid, A.I., Gaunt, S.J., 2002. Colinearity and non-colinearity in the expression of Hox genes in developing chick skin. Int. J. Dev. Biol. 46, 209–215.
Sauvageau, G., Thorsteinsdottir, U., Eaves, C.J., Lawrence, H.J., Largman, C., Lansdorp, P.M., Humphries, R.K., 1995. Overexpression of HOXB4 in hematopoietic cells causes the selective expansion of more primitive populations in vitro and in vivo. Genes Dev. 9, 1753–1765.
Sauvageau, G., Iscove, N.N., Humphries, R.K., 2004. In vitro and in vivo expansion of hematopoietic stem cells. Oncogene 23, 7223–7232.
Showell, C., Binder, O., Conlon, F.L., 2004. T-box genes in early embryogenesis. Dev. Dyn. 229, 201–218.
So, C.W., Karsunky, H., Wong, P., Weissman, I.L., Cleary, M.L., 2004. Leukemic transformation of hematopoietic progenitors by MLL-GAS7 in the absence of Hoxa7 or Hoxa9. Blood 103, 3192–3199.
Soriano, P., 1999. Generalized lacZ expression with the ROSA26 Cre reporter strain. Nat. Genet. 21, 70–71.
Spitz, F., Gonzalez, F., Peichel, C., Vogt, T.F., Duboule, D., Zakany, J., 2001. Large scale transgenic and cluster deletion analysis of the HoxD complex separate an ancestral regulatory module from evolutionary innovations. Genes Dev. 15, 2209–2214.
Stelnicki, E.J., Komuves, L.G., Kwong, A.O., Holmes, D., Klein, P., Rozenfeld, S., Lawrence, H.J., Adzick, N.S., Harrison, M., Largman, C., 1998. HOX homeobox genes exhibit spatial and temporal changes in expression during human skin development. J. Invest Dermatol. 110, 110–115.
Suemori, H., Noguchi, S., 2000. Hox C cluster genes are dispensable for overall body plan of mouse embryonic development. Dev. Biol. 220, 333–342.
Tarchini, B., Duboule, D., Kmita, M., 2006. Regulatory constraints in the evolution of the tetrapod limb anterior–posterior polarity. Nature 443, 985–988.
Thorsteinsdottir, U., Sauvageau, G., Hough, M.R., Dragowska, W., Lansdorp, P.M., Lawrence, H.J., Largman, C., Humphries, R.K., 1997. Overexpression of HOXA10 in murine hematopoietic cells perturbs both myeloid and lymphoid differentiation and leads to acute myeloid leukemia. Mol. Cell Biol. 17, 495–505.
Thorsteinsdottir, U., Mamo, A., Kroon, E., Jerome, L., Bijl, J., Lawrence, H.J., Humphries, K., Sauvageau, G., 2002. Overexpression of the myeloid leukemia-associated Hoxa9 gene in bone marrow cells induces stem cell expansion. Blood 99, 121–129.
Wellik, D.M., Capecchi, M.R., 2003. Hox10 and Hox11 genes are required to globally pattern the mammalian skeleton. Science 301, 363–367.
Wilson, A., MacDonald, R.H., Radtke, F., 2001. Notch 1-deficient common lymphoid precursors adopt a B cell fate in the thymus. J. Exp. Med. 194, 1003–1012.
Young, T., Rowland, J.E., Van, D.V., Bialecka, M., Novoa, A., Carapuco, M., van Nes, J., de Graaff, W., Duluc, I., Freund, J.N., Beck, F., Mallo, M., Deschamps, J., 2009. Cdx and Hox genes differentially regulate posterior axial growth in mammalian embryos. Dev. Cell 17, 516–526.
Zacchetti, G., Duboule, D., Zakany, J., 2007. Hox gene function in vertebrate gut morphogenesis: the case of the caecum. Development 134, 3967–3973.
Zakany, J., Duboule, D., 1999. Hox genes and the making of sphincters. Nature 401, 761–762.
Zakany, J., Kmita, M., Alarcon, P., de la Pompa, J.L., Duboule, D., 2001. Localized and transient transcription of Hox genes suggests a link between patterning and the segmentation clock. Cell 106, 207–217.
Zhao, Y., Potter, S.S., 2002. Functional comparison of the Hoxa 4, Hoxa 10, and Hoxa 11 homeoboxes. Dev. Biol. 244, 21–36.